# Accepted Manuscript


Facile synthesis, structural evaluation, antimicrobial activity and synergistic effects of novel imidazo[1,2-*a*]pyridine based organoselenium compounds

Sanjeev Kumar, Nidhi Sharma, Indresh K. Maurya, Aman K. Bhasin, Nishima Wangoo, Paula Brandão, Vítor Félix, K.K. Bhasin, Rohit K. Sharma

PII: S0223-5234(16)30641-9

DOI: 10.1016/j.ejmech.2016.07.076

Reference: EJMECH 8794

To appear in: *European Journal of Medicinal Chemistry*

Received Date: 6 June 2016

Revised Date: 28 July 2016

Accepted Date: 31 July 2016

Please cite this article as: S. Kumar, N. Sharma, I.K. Maurya, A.K. Bhasin, N. Wangoo, P. Brandão, V. Félix, K.K. Bhasin, R.K. Sharma, Facile synthesis, structural evaluation, antimicrobial activity and synergistic effects of novel imidazo[1,2-*a*]pyridine based organoselenium compounds, *European Journal of Medicinal Chemistry* (2016), doi: 10.1016/j.ejmech.2016.07.076.

# Graphical Abstract

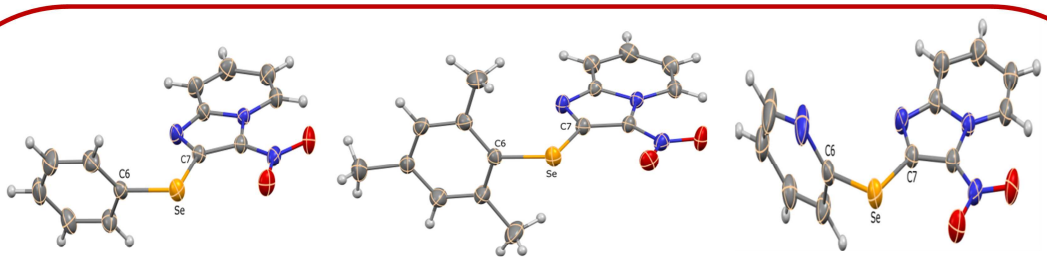

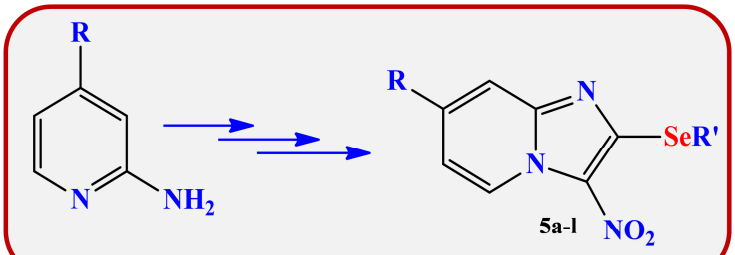


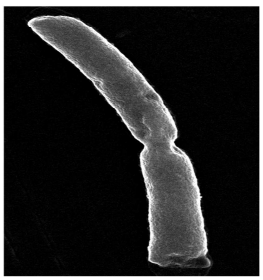

*E. coli. treated*
**with 5a (2.48µg/ml)**

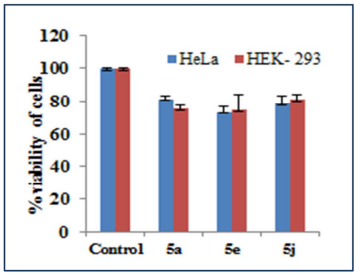


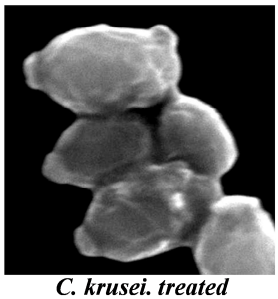

*C. krusei. treated*
**with 5e (9.96 µg/ml)**

# Facile synthesis, structural evaluation, antimicrobial activity and synergistic effects of novel imidazo[1,2-*a*]pyridine based organoselenium compounds

*Sanjeev Kumar* [a], *Nidhi Sharma* [a], *Indresh K. Maurya* [b], *Aman K. Bhasin* [a], *Nishima Wangoo* [c], *Paula Brandão* [d], *Vítor Félix*[d,e], *K. K. Bhasin* [a,]*, *and Rohit K. Sharma*[a,]*

[a]Department of Chemistry & Centre for Advanced Studies in Chemistry, Panjab University, Chandigarh, 160014 India

[b]Department of Microbial Biotechnology, Panjab University, Chandigarh, 160014 India

[c]Department of Applied Sciences, University Institute of Engineering & Technology (U.I.E.T), Panjab University, Chandigarh, 160014 India

[d]Department of Chemistry, CICECO – Aveiro Institute of Materials, University of Aveiro, 3810-193 Aveiro, Portugal

[e]Department of Medical Sciences, iBiMED – Institute of Biomedicine, University of Aveiro, 3810-193 Aveiro, Portugal

*****Corresponding authors

**(**R.K.S.) Tel: +91 172 2534409. E-mail: rohitksg@pu.ac.in

(K.K.B) Tel: +91 172 2534407. E-mail: kkbhasin@pu.ac.in

**ABSTRACT:** A simple and efficient method has been described to synthesize the hitherto unknown imidazo[1,2-*a*]pyridine selenides (**5a-l**) by reaction of 2-chloroimidazo[1,2-a]pyridines with aryl/heteroaryl selenols, generated in situ by reduction of various diselenides with hypophosphorous acid. The crystal structures of 3-nitro-2-(phenylselanyl)-imidazo[1,2-*a*]pyridine (**5a**), 2-(mesitylselanyl)-3-nitro-imidazo[1,2-*a*]pyridine (**5d**) and 3-nitro-2-(pyridin-2-ylselanyl)-imidazo[1,2-*a*]pyridine (**5e**) were confirmed by X-ray crystallography and the DFT calculations were performed to determine various structural parameters which were correlated with the X-ray crystal structures. The synthesized compounds were subjected to antimicrobial evaluation and it was found that compounds **5a** and **5j** were active against gram negative bacterium *E. coli* whereas compound **5e** was active against different fungal strains. Time kill assay was performed to understand the microbial activity of synthesized organoselenium compounds and the toxicity of these compounds was evaluated against human cell lines. Synergistic effects of active compounds **5a** and **5e** were tested with existing antibiotic drugs which exhibited that the antibiotic combination with synthesized organoselenium compounds efficiently enhanced the antimicrobial activity.

## 1. Introduction

Organoselenium chemistry has been an area of continuous research since selenium and its compounds were identified as micronutrient for several bacteria, mammals and birds [1]. The relevance of organoselenium compounds has seen an upward thrust particularly after 1970's with discovery of many new attractive compounds with various important synthetic and biological applicability [2]. Several synthetic methods have been developed to synthesize organoselenium compounds till date, which generally include the use of expensive catalysts and various transition metals routinely employing harsh reaction conditions and long reaction times [3]. This has led to continuous search for finding better, inexpensive and environment friendly approaches for synthesis of organoselenium compounds. The recent efforts in this regard have yielded an efficient and eco-friendly method in absence of solvent under microwave irradiation to obtain selenoesters [4]. Similarly, the use of hypophosphorous acid in glycerol as an efficient environment friendly system for reducing diselenides in the preparation of monoselenides has also been described [5]. In another example, a metal free approach was followed to achieve synthesis of unsymmetrical selenides in different ionic liquids [6]. Moreover, unsymmetrical arylselanyl anilines have been reported to be synthesized under metal and base free conditions [7].

In context of the biological applications of organoselenium compounds, these have been reported to mimic the function of antioxidant selenoenzyme Glutathione peroxidase (Gpx) [8]. In a recent report, novel ebselenol compounds have been identified as multifunctional antioxidants with regenerable radical-trapping and enhanced hydroperoxide-decomposing capabilities [9]. Selenium has been found to be present in number of selenoproteins and enzymes as selenocysteine residue at the active site [10]. In fact, selenocysteine is found to be 21st proteinogenic amino acid which has active selenol group present in active site of Gpx and similar enzymes [10-11]. Despite the perceived toxicity aspects related to selenium based compounds, a number of selenium containing molecules are being developed as novel pharmacological agents [12-13] including anticancer [14,15], anti-inflammatory [16], antitumour [17] and membrane permeabilization [18] agents. The new age drugs such as Ethaselen (anticancer) and Ebselen (anti-inflammatory) contain selenium and are termed among the important discoveries in organoselenium and medicinal chemistry [19].

The application of selenium enriched compounds containing one or two heteroaromatic moieties have been observed to be more in biological systems compared to their non-heteroaryl analogues [12]. This observation is based on the experimental evidences which suggest that many heteroaryl moieties such as pyrimidine, pyridine, quinoline, imidazole, ferrocene, indole and pyrazole in association with selenium exhibit moderate to good biological results [20]. However, imidazo[1,2-*a*]pyridine, which is an aromatic heterocycle with bridgehead nitrogen atom [21], has not been sufficiently explored for applications resulting from conjugation with selenium, although chemistry of unconjugated imidazo[1,2-a]pyridine has been intensively investigated in last few decades [22]. Recently, solvent- and metal-free chalcogenation of imidazo[1,2-*a*]pyridines with regioselectivity at C-3 position has been effectively reported [23]. The imidazo[1,2-*a*]pyridine based compounds are of immense interest as these have been reported to be exhibiting wide range of biological effects, notably in form of antiviral, antifungal, antimalarial, antiparasitic, herbicide, anticancer, anti-inflammatory and antibacterial activities [24]. Keeping the focus on greener strategies for synthesis of organoselenium derivatives, herein we report the synthesis and applications of novel imidazo[1,2-*a*]pyridine based organoselenium compounds. To best of our knowledge, this is the first report describing the chemical synthesis, structural determination, computational analysis, antimicrobial evaluation and synergistic effects of novel nitro substituted imidazo[1,2-*a*]pyridine derived organoselenium compounds.

## 2. Results and discussions

### *2.1 Chemistry*

The synthetic route adopted for preparation of organoselenium compounds based on imidazo[1,2-*a*]pyridine herein is depicted in Scheme 1. Initially, 2-chloroimidazo[1,2-*a*]pyridine was synthesized in a two-step procedure from 2-aminopyridine which included the first step involving the condensation reaction of 2-aminopyridine with chloroacetic acid in the presence of triethylamine in water as a solvent to afford 2-(2-iminopyridin-1(2H)-yl)acetic acid (**2a**) [21]. Compound **2a** was further refluxed with phosphorous oxychloride to facilitate the intramolecular cyclisation for preparation of 2-chloroimidazo[1,2-*a*]pyridine (**3a**) in good yield. It was further observed that nucleophilic substitution of chlorine atom at C-2 position in **3a** is not entirely a feasible process as this position is not adequately nucleophilic in nature [25]. Moreover, the attack of nucleophile may not allowed either by $SN_1$ (as there is no driving force for chloride to leave by itself) or $SN_2$ mechanism (as the incoming nucleophile is unlikely to attack from inner

side of the five membered ring).Thus, the introduction an electron withdrawing group at C-3 position of substituted imidazo[1,2-*a*]pyridine (**3a-b**) seemed to be essential for facilitation of nucleophilic aromatic substitution of chlorine atom. Thus, nitration of compounds (**3a-b**) was carried out using nitric acid and sulphuric acid to afford nitro substituted imidazo[1,2-*a*]pyridine (**4a-b**) in excellent yields [26].

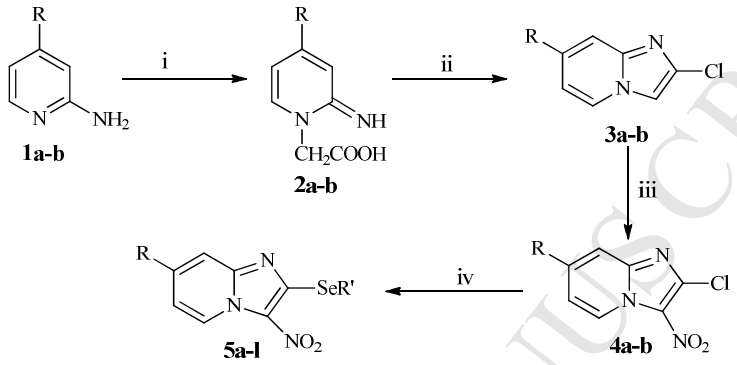


[a]Reagents and conditions: (i) $Et_3N$, $ClCH_2COOH$, $H_2O$, reflux, 5h, ethanol, 2h, 89% (ii) $POCl_3$, toluene, reflux, 16h, 72-74% (iii) $H_2SO_4$, $HNO_3$, 3h, 80-82% (iv) 0.5eq. $R'_2Se_2$, $H_3PO_2$, Ethanol, 74-91%

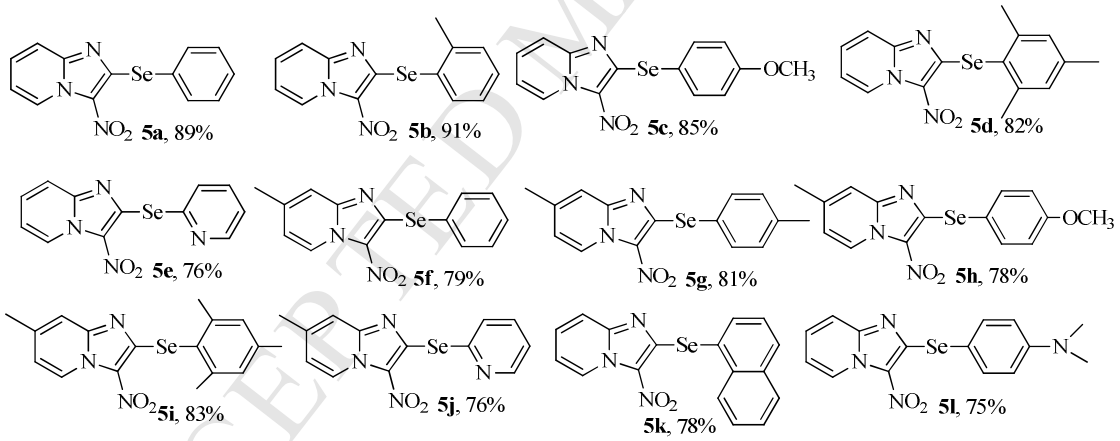


**Scheme 1.** Synthesis of organoselenium derivatives of imidazo[1,2-*a*]pyridines

A modified procedure of already reported method [5] was further used to cleave the Se-Se bond of diselenides to generate selenide anion which is sufficiently nucleophilic in nature to substitute chlorine atom of imidazo[1,2-*a*]pyridine (**4a-b**). In this modified procedure, ethanol was used as a solvent instead of glycerol to improve the yield in our case and also generating selenol at lower temperature ($60^0$C) as compared to earlier reported temperature conditions ($90^0$C). The versatility of the present multi-step synthetic approach was further evaluated by

using different diselenides [27] such as 2,2'-ditolyl diselenide, 4,4'-ditolyl diselenide, 4,4'-dianisyl diselenide, 2,2'-dimesityl diselenide, 2,2'-dipyridyl diselenide, 4,4'(*N*,*N*'-dimethylaniline) diselenide and dinaphthyl diselenide to yield desired compounds (**5a-l**). In addition, the reaction was also investigated with methyl substituted imidazo[1,2-*a*]pyridine which showed negligible effect on yield.

## 2.2 *Crystallographic studies*

The structures of compounds **5a**, **5d** and **5e** were determined by single crystal X-ray crystallography. Suitable single crystal of compounds **5a**, **5d** and **5e** were grown at room temperature in dichloromethane:hexane (30:70) by slow evaporation for X-ray diffraction. The crystal lattices of selenium derivatives **5a** and **5e** are built up from asymmetric unit composed of a single molecule. Views of asymmetric units of **5a**, **5d** and **5e** are shown in Fig. 1 (i, ii, iii respectively) with the relevant atomic labeling scheme adopted. The three molecular structures are overlapping apart the phenyl moieties, as depicted in Fig. 1(iv), the carbon atoms are shown in green (**5a**), cyan (**5d**) and magenta (**5e**), while the hydrogen, nitrogen and oxygen atoms are shown in white, blue and red, respectively In fact, the overlay between the nitro-substituted imidazo[1,2-*a*]pyridine moieties of **5a** with **5d** and **5e** leads to the root mean square deviations

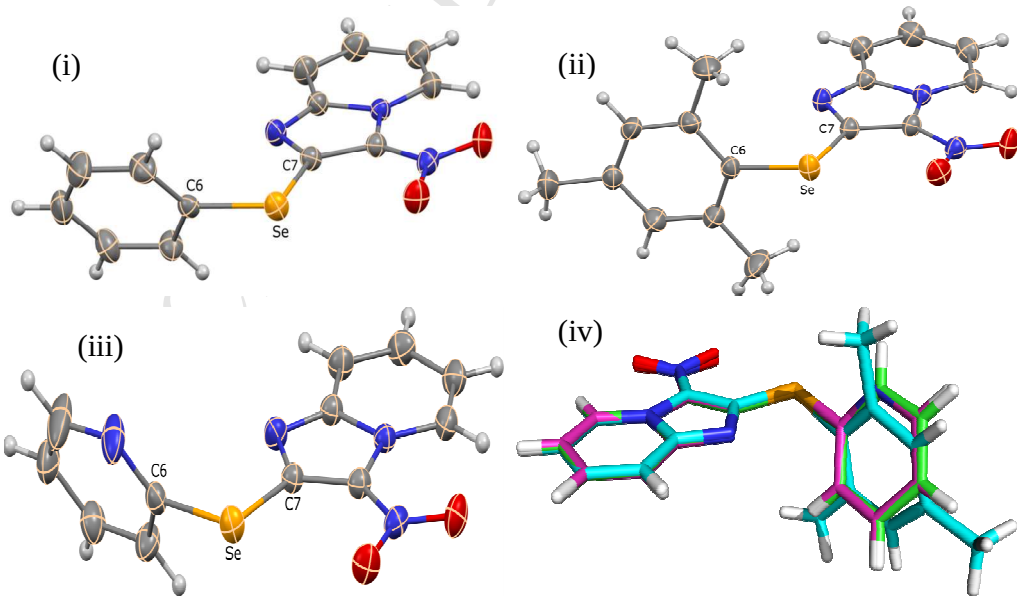


**Fig. 1.** Molecular diagrams of **5a** (i) **5d** (ii) and **5e** (iii) with thermal ellipsoids drawn at the 50% probability level, Overlap between **5a**, **5d** and **5e**(iv)

(RMSD) of only 0.049 and 0.067 Å, respectively whereas the RMSD between **5d** and **5e** is 0.058 Å. Furthermore, the dihedral angle between the phenyl ring and imidazo[1,2-*a*]pyridine moiety is similar in compounds **5a** (62.6$^{o}$) and **5e** (62.7$^{o}$).

In contrast, these two moieties adopt an almost orthogonal disposition in **5a** with a dihedral angle of 89.5$^{o}$, which is probably imposed by the minimization of steric interactions between the methyl phenyl substituents and the imidazole ring. In addition, packing effects, as depicted in Fig.1 (iv), can also affect the spatial disposition of the substituents around the selenium center. The bond lengths and bond angles involving the selenium center (from X-ray diffraction data)

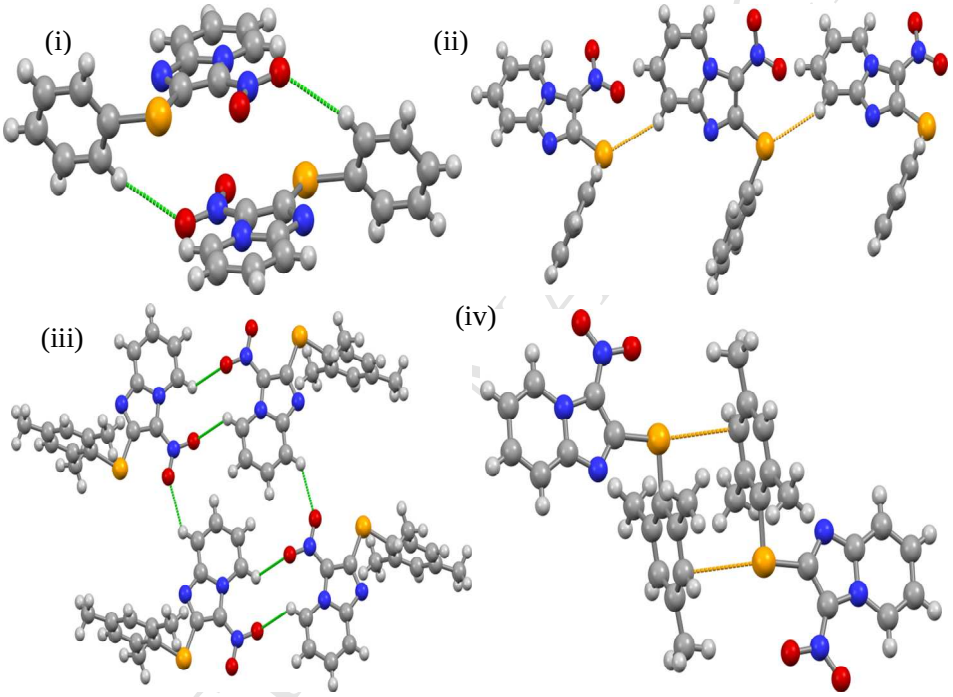


**Fig. 2.**Crystal packing features with the C–H···O bonds drawn as green dashed lines of **5a** (i) and **5d** (iii); and C–H···Se short contacts as yellow dashed linesof **5a** (ii) and **5d** (iv) respectively

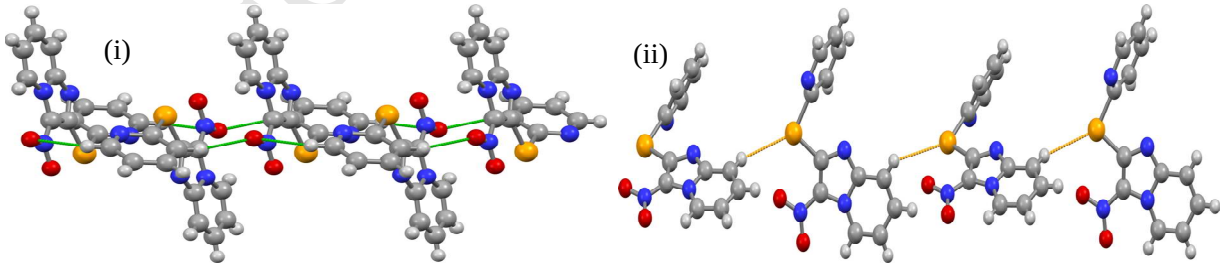


**Fig. 3.** Crystal packing features of **5e**, with the C–H···O bonds drawn as green dashed lines (i) and C–H··Se short contacts as yellow dashed lines (ii).

are listed in Table 1. In all the three crystals, it is consistently observed that Se-C6 bond length to the phenyl group is slightly longer than Se-C7 bond length to the imidazo[1,2-*a*]pyridine moiety. This may be explained on basis of electron withdrawing ability of nitro group which in turn is attached at C15 position of imidazo[1,2-*a*]pyridine rendering the Se-C7 bond shorter than the usual length. The most relevant intermolecular interactions observed in the crystal structures of compounds **5a**, **5d** and **5e** are C–H···O hydrogen bonds followed by C–H···Se short contacts in compounds **5a** and **5e**, and C···Se in **5d**. In the crystal structure of compound **5a**, the molecules

**Table 1.** Comparison between theoretical and experimental bond parameters around Se atom in **5a**, **5d** and **5e**

| | X-ray crystallography | | | Theoretical calculation | | |
|---|---|---|---|---|---|---|
| | Bond length (Å) | | | | | |
| | **5a** | **5d** | **5e*** | **5a** | **5d** | **5e*** |
| Se-C6 | 1.916 | 1.932 | 1.930 | 1.932 | 1.934 | 1.939 |
| Se-C7 | 1.883 | 1.880 | 1.885 | 1.886 | 1.882 | 1.885 |
| | Bond Angle (°) | | | | | |
| C6-Se-C7 | 97.0 | 97.8 | 96.56 | 97.8 | 98.7 | 105.3 |
| Se-C6-C1 | 120.4 | 120.4 | 115.9 | 119.8 | 119.2 | 107.4 |
| Se-C6-C5 | 119.4 | 118.6 | 120.2 | 119.8 | 119.0 | 128.7 |
| Se-C7-N8 | 124.2 | 124.4 | 123.9 | 124.4 | 124.1 | 126.8 |

*C1=N1 for **5e**

are self-assembled in dimers (Fig. 2 (i)), through two C–H···O hydrogen with O···C distance of 2.885(2) Å and a C–H···O angle of 114°.In compound **5d**, 1-D network of C–H···O hydrogen bonding interactions are constructed from a centro-symmetric motif composed of four molecules linked by six hydrogen bonds with O···C distances of 3.172(2) Å and 3.229(2) Å and C–H···O angles of 134° and 126°, respectively (Fig. 2 (iii)). The crystal structure of **5e** also exhibits a 1-D network of C–H···O hydrogen bonding interactions with C···O distances of 3.322(3) and 3.466(2) Å. In addition, adjacent molecules are disposed in an anti-parallel disposition (Fig. 3 (i)). The crystal structures of **5a** and **5e** display C–H···Se short contacts with H···Se distances of 3.053 and 3.067 Å, respectively, leading to the formation of a C–H···Se 1-D network of contacts

(Fig. 2 (ii) and Fig. 3 (ii)). On the other hand, neighboring molecules of compound **5d**, adopting an antiparallel disposition are separated by short C···Se contacts of 3.369 Å (Fig. 2 (iv)).

*2.3 Theoretical study*

The gas phase structures of synthesized compounds **5a-l** were optimized (Supporting Information, Table S2) using density functional theory (DFT) and employing Becke's three parameter exchange functional (B3) in conjunction with the correlation functional proposed by Lee, Yang and Parr (LYP) and 6-31 G(d) basis set (B3LYP/6-31G(d) [28]. The calculated Se-C and Se-C7 distances in compounds **5a**, **5d** and **5e** are in good agreement with those obtained from their crystal structures (Table 1). Also, the calculated C-Se-C bond angle in compounds **5a** and **5d** is in close proximity to that obtained from corresponding crystal structure while in the compound **5e**; this angle was observed to be slightly lower in crystal structure. The probable reason for this slight deviation may be crystal packing effects.

**Table 2.** C-Se bond lengths (Å) and C-Se-C angle (º) together with HOMO and LUMO energies of **5a-l** calculated using B3LYP/6-31G(d)

| | Se-C6 (Å) | Se-C7 (Å) | C6-Se-C7 (°) | HOMO (a. u.)* | LUMO (a. u.) | Energy Gap (eV) |
|---|---|---|---|---|---|---|
| **5a** | 1.932 | 1.886 | 97.81 | -0.22404 | -0.08134 | 3.883 |
| **5b** | 1.934 | 1.884 | 98.50 | -0.22274 | -0.08175 | 3.836 |
| **5c** | 1.929 | 1.887 | 98.07 | -0.22386 | -0.08103 | 3.886 |
| **5d** | 1.934 | 1.882 | 98.73 | -0.21961 | -0.08013 | 3.795 |
| **5e** | 1.939 | 1.885 | 105.25 | -0.21813 | -0.08595 | 3.596 |
| **5f** | 1.932 | 1.886 | 97.95 | -0.22152 | -0.07756 | 3.917 |
| **5g** | 1.929 | 1.887 | 98.00 | -0.22000 | -0.07646 | 3.906 |
| **5h** | 1.929 | 1.887 | 97.84 | -0.22138 | -0.07724 | 3.922 |
| **5i** | 1.935 | 1.883 | 98.60 | -0.21703 | -0.07687 | 3.814 |
| **5j** | 1.938 | 1.885 | 105.20 | -0.21590 | -0.08219 | 3.638 |
| **5k** | 1.933 | 1.899 | 100.55 | -0.20603 | -0.08460 | 3.304 |
| **5l** | 1.920 | 1.888 | 98.59 | -0.19478 | -0.07545 | 3.247 |

*1 a. u. = 27.212eV

The calculated Se-C bond of all the synthesized compounds (**5a-l**) have been reported in Table 2 together with energy values of highest occupied molecular orbital (HOMO) and lowest unoccupied molecular orbital (LUMO). The C6-Se bond length was found to be in the range of 1.929-1.939 Å and C7-Se bond length between 1.882-1.899 Å, with both in agreement with the experimental values observed for compounds **5a**, **5d** and **5e** in crystal state. The phenyl, tolyl and anisyl substituted imidazo[1,2-a]pyridine selenides (**5a-c**, **5f-h**) had higher HOMO-LUMO gap as compared to pyridine, mesityl, naphthyl substituted selenides (**5d-e**, **5i-l**). A general probable reason for such an observation is that electron withdrawing groups on phenyl ring tend to stabilize HOMO thereby lowering its energy while keeping the LUMO energy almost unchanged whereas electron donating groups tend to destabilize the HOMO state and augment its energy. The HOMO of compound **5d** with three methyl (electron donating) groups on phenyl ring is higher in energy than compounds **5a**, **5b** and **5c** (with lesser or no electron donating groups). For similar reasons, the energy gap of derivative **5i** (R= $CH_3$, R'= mesityl) is less than corresponding compounds **5f**, **5g** and **5h** (R'= phenyl, tolyl, anisyl). Also, the presence of methyl group on imidazo[1,2-*a*]pyridine ring system slightly increases the energy gap compared to unsubstituted system because of more destabilization of LUMO than HOMO (Table 2). In case of pyridyl substituted imidazo[1,2-*a*]pyridine selenides (**5e**, **5j**)large stabilization of LUMO was observed which makes HOMO and LUMO to come closer and thereby decreasing the energy gap considerably. For compounds **5a-j**, HOMO is mainly composed of imidazo[1,2-*a*]pyridine ring system (Supporting Information, Fig. S2), however, compounds **5k** and **5l** have naphthyl and N, N'-dimethylphenyl moieties as the major contributors towards HOMO, respectively (Supporting Information, Fig. S3). This is one of the main reasons for the relatively large destabilization of HOMO and also stabilization of LUMO subsequently decreasing the energy gap.

*2.4 Antimicrobial Activity*

The synthesized compounds (**5a-l**) were evaluated for antimicrobial activities against different bacterial and fungal strains (Supporting Information, Table S3-S4). In this context, the synthesized derivatives **5a** (R = H; R' = phenyl) and **5j** (R = $CH_3$; R' = pyridyl) were observed to exhibit antibacterial activity with MIC value 2.48 µg/ml and 10.41 µg/ml respectively against Gram-negative bacteria *E. coli* (Table 3). These observed activities, in particular the one observed for compound **5a** against *E. coli*, have been found to be more potent as compared to the

few reports concerning antimicrobial activity of selenide based compounds in literature so far [29] and quite similar to the Rifampicin (standard).However, in case of activity against tested fungal strains, only compound **5e** was found to be exhibiting multi-spectrum activity against *A. fumigates*, *C. krusei*, *A. niger*, and *C. parapsilosis* with observed MIC values of 9.96, 9.96,19.93 and 19.93 µg/ml respectively (Table 3).

**Table 3.** Antibacterial and antifungal activities of compounds **5a**, **5e** and **5j** [in MIC[b] (µg/ml)]

| Compound | *E. coli*[a] | *A. fumigatus*[a] | *C. krusei*[a] | *A. niger*[a] | *C. parapsilosis*[a] |
|---|---|---|---|---|---|
| **5a** | 2.48 | >39.77 | >39.77 | >39.77 | >39.77 |
| **5e** | >39.89 | 9.96 | 9.96 | 19.93 | 19.93 |
| **5j** | 10.41 | >41.66 | >41.66 | >41.66 | >41.66 |

[a] Standard used: Rifampicin (MIC = 1.02 µg/ml for *E. coli*); Amphotericin B (MIC = 0.18 µg/ml for *A. fumigatus*, MIC = 0.36 µg/ml for *C. krusei*, MIC = 0.18 µg/ml for *A. niger*, MIC = 0.18 µg/ml for *C. parapsilosis*). [b] MIC: Minimum Inhibitory Concentration

*2.4.1 Cytotoxicity*

The toxicity effect of the three active relatively active compounds (**5a**, **5e**, **5j**) was evaluated to determine their safety profile against HEK-293 and HeLa cells at their MIC values. The compounds **5a**, **5e**, and **5j** were found to exhibit less than 25% toxicity against both HeLa and HEK-293 cells (Fig. S1). Considering the toxicity issues concerning some of the earlier reported organoselenium analogues, the presently compounds have demonstrated acceptable mammalian cytotoxicity that is further authenticated by calculating selectivity index (SI) of the active compounds, which is described as theratio of cytotoxicity to biological activity (SI = CC50 of HEK-293 or HeLa/IC50 of microorganisms) of compounds against microorganisms were calculated. Notably all the three compounds (**5a**, **5e** and **5j**) with antimicrobial activity (MIC) against *E. coli* [2.48 µg/ml (**5a**), 10.41 µg/ml (**5j**)] and *C. krusei* [9.96 µg/ml (**5e**)], *A. fumigates* [9.96 µg/ml (**5e**)], possess good selectivity index against HeLa cells [4.46 (**5a**), 3.80 (**5e)** and 3.87 (**5j**)] and HEK-293 cells [5.57 (**5a)**, 3.60 (**5e)** and 4.60 (**5j**)]. (Supporting Information, Table S5).

*2.4.2 Time kill assay*

Further, to account for the efficacy of active compounds, the time kill kinetic studies were performed in which colony forming units (CFUs) of the *E. coli* and *C. krusei* were rapidly reduced after treatment with compounds **5a** (at MIC = 2.48 µg/ml) and **5e** (at MIC = 9.96 µg/ml), respectively (Fig. 4). It was observed that the maximum killing of *E. coli and C. krusei* cells with compounds **5a** and **5e** respectively, were observed after about 20 h in comparison to the used control. Therefore, it can be safely interpreted that the compound **5a** is successfully inhibiting the growth of the Gram negative bacterium *E. coli* and the same effect is being pronounced upon by compound **5e** against the fungal strain *C. krusei*.

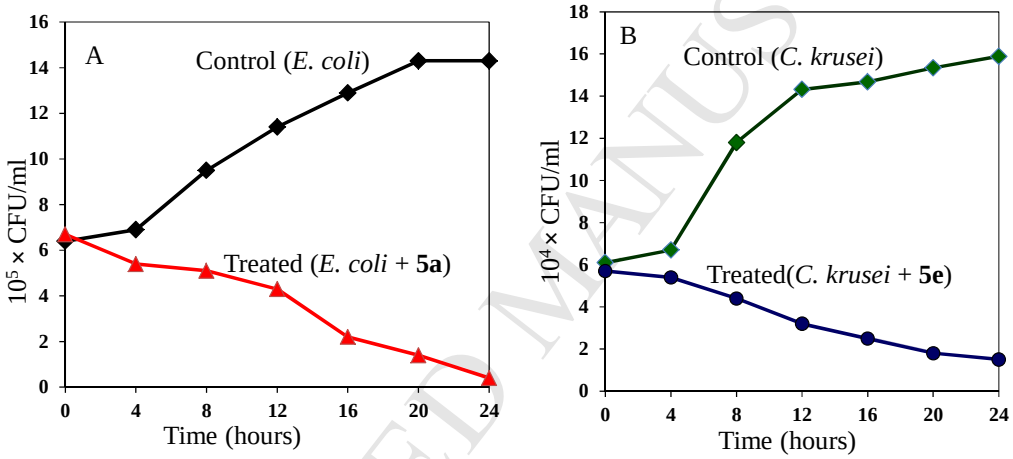


**Fig. 4.**Time Kill assay of compound **5a** against *E. coli* (A) and compound **5e** against *C. krusei* (B)

*2.4.3 FE-SEM analysis*

The morphological effects of active compounds **5a** and **5e** on the *E. coli* and *C. krusei* respectively were investigated using Field Emission Scanning Electron Microscopy (FE-SEM). A change in both *E. coli* and *C. krusei* cell morphology was observed when treated with **5a** and **5e** at their MIC value. Increased roughness and damage of the cell wall was observed after 2h of incubation which confirmed the antimicrobial effect of the tested active compounds (Fig. 5).

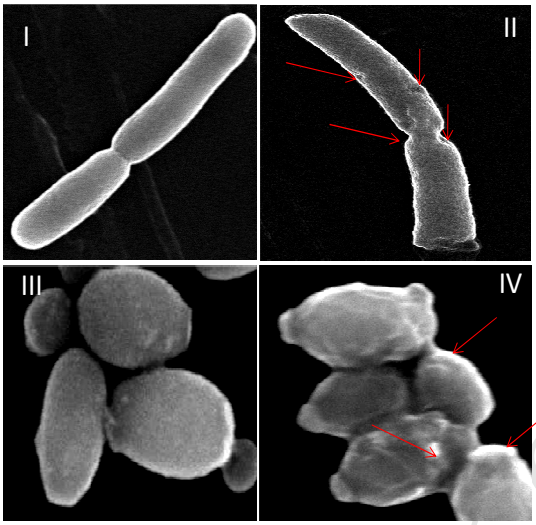


**Fig. 5.** FE SEM images of (I) Control cells (*E. coli*, 15000X, 8.1mm); (II) **5a** treated *E. coli* cells (15000X, 8.1mm); (III) Control (*C. krusei*, 7500X, 20mm); (IV) **5e** treated C. krusei cells (7500X, 20mm)

*2.4.4 Synergy*

The evaluation of combinations of new lead compounds and existing antibiotics is an effective way of enhancing theantimicrobial potency. Keeping this in mind, *in vitro* efficacies of compounds **5a** and **5e** were evaluated by checker board dilution assay with well-known antibacterial drugs suchas kanamycin (KAN), Rifampicin (RIF) and antifungal drugs Amphotericin B (Amp B) and Fluconazole (FLC) against *E. coli* and *C. krusei* respectively (Table 4). Interestingly, the synergistic results with known drugs showed much better antimicrobial efficacies at less dosage. The fractional inhibitory concentration index [FICI = (MIC of drug in combination/MIC of drug alone) + (MIC of the tested compound in combination/MIC of the tested compound alone) and considered to be synergistic if value of FICI $\leq$ 0.5], was determined for combinations of concentrations.

**Table 4.** Synergistic studies of compounds **5a** and **5e** with known antibiotics against *E. coli* and *C. krusei* respectively

| MIC(μg/ml) | MIC(μg/ml) | MIC(μg/ml) | FICI | Effect |
|---|---|---|---|---|
| **KAN** | **5a** | **KAN + 5a** | 0.370 | Synergy |
| 0.58 | 2.48 | 0.07 + 0.62 | | |
| **RIF** | **5a** | **RIF + 5a** | 0.175 | Synergy |
| 1.02 | 2.48 | 0.052 + 0.31 | | |
| **Amp B** | **5e** | **Amp B + 5e** | 0.372 | Synergy |
| 0.18 | 9.96 | 0.022 + 2.49 | | |
| **FLC** | **5e** | **FLC + 5e** | 0.623 | No Synergy |
| 0.03 | 9.96 | 0.0037+4.98 | | |

The corresponding results for compound **5a** showed effective synergy with antibacterial drugs (KAN, RIF) WITH FICI = 0.37 for KAN and FICI = 0.175 for RIF in inhibiting *E. coli* growth. Further, the combination of non-cidal concentration of **5a** resulted in potentiating of KAN by 8 fold (MIC of 0.58 μg/ml to 0.07 μg/ml) and RIF by ~20 fold (MIC of 1.02 μg/ml to 0.052 μg/ml) against *E. coli* (Table 4). Similarly, the compound **5e** also demonstrated synergistic effect with antifungal drug Amp B with FICI = 0.372 in inhibiting *C. krusei* growth. The MIC for Amp B was lowered by ~8 fold with **5e** (MIC of 0.18 to 0.022 μg/ml) against *C. krusei*. Instead, compound **5e** does not exhibit same kind of synergistic effect with FLC with the observed FICI value of 0.623 although the MIC for FLC was lowered by 8 fold with **5e** (MIC of 0.03 μg/ml to 0.0037 μg/ml) against *C. krusei* (Table 4).

## 3. Conclusions

An efficient route for the synthesis of organoselenium compounds based on heterocyclic moiety imidazo[1,2-a]pyridine has been developed and reported herein. The selenylation of imidazo[1,2-a]pyridine at its C-2 position has been carried out leading to the formation of compounds **5a-l**. The use of hypophosphorous acid in selenol generating step provides advantage over conventional methods in terms of greener and metal free conditions. Out of all synthesized compounds, three derivatives **5a**, **5d** and **5e** have been thoroughly characterized using X-ray crystallography. The theoretical optimization of synthesized compounds (**5a-l**) was performed to

understand their three dimensional structure and effect of different structural substitutions on the HOMO-LUMO energy levels. The single crystal X-ray structure parameters were found to be in acceptable close agreement with theoretically generated values. Further, the synthesized compounds were biologically evaluated against a host of bacterial and fungal strains leading to demonstration of broad spectrum of activities against few of them. Specifically, compounds **5a** (2.48 µg/ml against *E. coli.*), **5j** (10.41 µg/ml against *E. coli.*) and **5e** (9.96 µg/ml against both *A. fumigates* and *C. krusei*) were found be exhibiting potent MIC values against listed strains. As the selenium based derivatives generally generate lot of curiosity regarding their toxicity, the safety profile of synthesized compounds exhibiting antimicrobial activity was evaluated by performing cytotoxicity studies against HEK-293 and HeLa cells which revealed that the tested compounds exhibited acceptable cytotoxicity. This was further confirmed by the good selectivity index values obtained against *E. coli* (with **5a**, **5j**) and *C. krusei* (with **5e**) in comparison to the tested HEK-293 and HeLa cells clearly indicating the selective action of these compounds against the micro-organisms versus mammalian cells. The microbial action of compounds **5a** and **5e** was further explored through time kill assay studies giving more meaningful measurement of antimicrobial activity. FE-SEM analysis also confirmed the morphological dissociation of bacterial and fungal cell membrane on treatment with tested compounds **5a** and **5e** on the *E. coli* and *C. krusei* respectively. Synergistic investigations of combinations of the most potent compounds **5a** and **5e** with existing antibiotics were performed to understand the effect on antimicrobial potency. In this respect, the FICI values obtained for these studies clearly suggested that compound **5a** exhibited enhanced synergy with Kanamycin and Rifampicin, and similar effect was noted for compound **5e** with Amphotericin B. Thus, considering the antimicrobial activity along with enhanced synergistic effects and relatively low toxicity, the reported organoselenium compounds serve as good candidates for usage as lead compounds for novel antimicrobials alone as well as in combination with known antibiotics.

## 4. Experimental Section

### *4.1 Chemistry*

All the experimental procedure involving selenium was carried out in dry and oxygen free nitrogen atmosphere. All the solvents used were dried and purified prior to use. Selenium (Sigma Aldrich, purity >99.0%) was purchased and stored in dessicator prior to use. Hypophosphorous acid, (SDFCL, 50% wt % in $H_2O$) was used as received and all the diselenide used were

prepared as per the reported method.[55] Column chromatography was performed using silica gel (99%, 60-120 mesh). $^{1}H$ and $^{13}C$ NMR spectra were recorded on a Bruker Avance II 400 MHz spectrophotometer in $CDCl_3$ or DMSO-$d_6$. $^{77}Se$ NMR was recorded on Bruker BioSpin GmbH operating at 76.31MHz. Infrared spectra were obtained on a Thermo Scientific Fisher spectrometer and mass spectrometry was carried out using Waters Q-TOFF micromass whereas Field Emission Scanning Electron Microscopy (FE-SEM) was performed on a Hitachi, SU8010 electron microscope, operating at 10-15kV

4.1.1 *General procedure for synthesis of selenides* (**5a-l**):

Hypophosphorous acid, 50 wt% in water (0.2 ml) was added to a solution of diaryl diselenide (1.0 mmol) in ethanol (25ml) under inert atmosphere, the resulting solution was refluxed for 30min changing color from yellow to colorless. After this reaction was cooled to room temperature followed by addition of corresponding imidazo[1,2-*a*]pyridine (**4a-b**) (2.0 mmol), stirred at $60^0$C till completion of reaction as monitored by thin layer chromatography (TLC). After that reaction mixture was poured into water and extracted with ethyl acetate (3x15ml), dried over $Na_2SO_4$ and concentrated in vacuo. The residue was purified by column chromatography (hexane/ethyl acetate, 5:1 (v/v)) to give product **5a** (89%).

*4.1.2 2-(Phenylselanyl)-3-nitro-imidazo[1,2-a]pyridine (**5a**):* Yield: 89%, yellow solid, m.p.: $177^0$C, δ (ppm): 9.40 (d, *J* = 6.9 Hz, 1H), 7.77 (dd, *J* = 7.4 Hz, *J* = 1.5 Hz, 2H), 7.60 – 7.54 (m, 2H), 7.47 – 7.42 (m, 3H), 7.20 – 7.16 (m, 1H); $^{13}C$ NMR (100MHz, $CDCl_3$) δ (ppm): 151.6, 147.3, 136.3, 131.3, 129.4, 127.6, 125.7, 117.1, 115.6; ); $^{77}Se$ NMR (76.31MHz, $CDCl_3$) δ (ppm): 453.9; IR (neat, ν $cm^{-1}$) 1629, 1452, 1379, 1327, 1123, 921, 736, 430. ES-MS: m/z 319.9 $[M+H]^+$

*4.1.3 2-(o-Tolylselanyl)-3-nitro-imidazo[1,2-a]pyridine (**5b**):* Yield: 91%, yellow solid, m.p.: $200^0$C, $^{1}H$ NMR (400 MHz, $CDCl_3$/DMSO-$d_6$) δ (ppm): 9.44 (d, *J* = 6.9 Hz, 1H), 7.79 (d, *J* = 7.4 Hz, 1H), 7.60 – 7.53 (m, 2H), 7.42 (dd, *J* = 4.9, 2.1 Hz, 2H), 7.24 (dt, *J* = 5.8 Hz, *J* = 2.3 Hz, 1H), 7.18 (td, *J* = 6.7, 1.8 Hz, 1H), 2.49 (s, 3H); $^{13}C$ NMR (100 MHz, $CDCl_3$/DMSO-$d_6$) δ (ppm): 151.5, 147.4, 143.3, 137.7, 131.2, 130.5, 130.3, 127.6, 126.7, 117.1, 115.4, 23.0; IR (neat, ν $cm^{-1}$) 3099, 1627, 1458, 1375, 1315, 1120, 921, 736, 433ES-MS: m/z 334.0 $[M+H]^+$

*4.1.4 2-(p-Methoxyphenylselanyl)-3-nitro-imidazo[1,2-a]pyridine (**5c**):* Yield: 85%, yellow solid, m.p.: $152^0$C, $^{1}H$ NMR (400 MHz, $CDCl_3$) δ (ppm): 9.42 (d, *J* = 6.9 Hz, 1H), 7.69 – 7.65

(m, 2H), 7.62 – 7.56 (m, 2H), 7.18 (td, *J* = 6.8 Hz, *J* = 1.5 Hz, 1H), 6.97 (d, *J* = 8.8 Hz, 2H), 3.86 (s, 3H). $^{13}$C NMR (100 MHz, $CDCl_3$) δ(ppm): 160.6, 152.4, 147.3, 137.9, 131.6, 131.2, 127.6, 117.8, 117.2, 117.1, 116.0, 115.5, 115.1, 55.3; IR (neat, ν $cm^{-1}$) 2961, 1628, 1449, 1375, 1320, 1127, 935, 747,437 ES-MS: m/z 350.0 $[M+H]^+$

*4.1.5 2-(Mesitylselanyl)-3-nitro-imidazo[1,2-a]pyridine (**5d**):* Yield: 82%, yellow solid, m.p.: 178$^0$C, $^1$H NMR (400 MHz, $CDCl_3$) δ (ppm): 9.35 (d, *J* = 6.9 Hz, 1H), 7.47 (q, *J* = 8.4 Hz, 2H), 7.08 (td, *J* = 6.8 Hz, *J* = 1.5 Hz, 1H), 6.96 (s, 2H), 2.38 (s, 6H), 2.26 (s, 3H); $^{13}$C NMR(100MHz, $CDCl_3$) δ(ppm): 151.8, 147.4, 143.7, 139.9, 131.1, 128.9, 127.7, 124.4, 117.0, 115.3, 24.1, 21.2; IR (neat, ν $cm^{-1}$) 2912, 1626, 1453, 1369, 1128, 935, 747, 437 ES-MS: m/z 362.0 $[M+H]^+$

*4.1.6 2-(Pyridin-2-ylselanyl)-3-nitro-imidazo[1,2-a]pyridine (**5e**):* Yield: 76%, orange red solid, m.p.: 162$^0$C, $^1$H NMR (400 MHz, DMSO-$d_6$) δ (ppm): 9.41 (d, *J* = 6.9 Hz, 1H), 8.57 (dd, *J* = 4.8 Hz, *J* = 1.1 Hz, 1H), 8.20 (d, *J* = 7.9 Hz, 1H), 7.82 (td, *J* = 7.7 Hz, *J* = 1.9 Hz, 1H), 7.77–7.76 (m, 2H), 7.43–7.36 (m, 2H); $^{13}$C NMR(100MHz, $CDCl_3$/DMSO-$d_6$) δ(ppm): 151.8, 149.7, 148.8, 146.8, 136.8, 132.2, 130.5, 127.6, 123.1, 116.5, 116.2; IR (neat, ν $cm^{-1}$) 1629, 1569, 1466, 1444, 1380, 1208, 1129, 922, 577, 430 ES-MS: m/z 321.2 $[M+H]^+$

*4.1.7 2-(Phenylselanyl)-7-methyl-3-nitro-imidazo[1,2-a]pyridine (**5f**):* Yield: 79%, light yellow solid, m.p.: 141$^0$C, $^1$H NMR (400 MHz, DMSO-$d_6$) δ (ppm): 9.20 (d, *J* = 7.0 Hz, 1H), 7.73 (d, *J*= 6.5 Hz, 2H), 7.49 (s, 1H), 7.47 – 7.42 (m, 3H), 7.18 (d, *J* = 6.8 Hz, 1H), 2.45 (s, 3H); $^{13}$C NMR(100MHz, $CDCl_3$/DMSO-$d_6$) δ(ppm): 150.4, 147.1, 144.0, 135.8, 129.0, 128.9, 128.7, 126.7, 125.6, 118.0, 115.4, 21.0; IR (neat, ν $cm^{-1}$) 2916, 1635, 1469, 1374, 1323, 1144, 891, 735, 465 ES-MS: m/z 334.0 $[M+H]^+$

*4.1.8 2-(4-Methylphenylselanyl)-7-methyl-3-nitro-imidazo[1,2-a]pyridine (**5g**):* Yield: 81%, yellow solid, m.p.: 165$^0$C, $^1$H NMR (400 MHz, $CDCl_3$/DMSO-$d_6$) δ (ppm): 9.19 (d, *J* = 7.0 Hz, 1H), 7.59 (d, *J* = 8.0 Hz, 2H), 7.52 (s, 1H), 7.25 (d, *J* = 7.9 Hz, 2H), 7.21 (dd, *J* = 7.0 Hz, *J* = 1.5 Hz, 1H), 2.44 (s, 3H), 2.39 (s, 3H); $^{13}$C NMR (100MHz, $CDCl_3$/DMSO) δ(ppm): 150.8, 147.1, 144.2, 138.8, 135.9, 129.8, 126.9, 122.0, 119.5, 118.1, 115.9, 115.3 20.9, 20.8; IR (neat, ν $cm^{-1}$) 2961, 1636, 1457, 1322, 1145, 851, 737, 486, 405 ES-MS: m/z 348.2 $[M+H]^+$

*4.1.9 2-(4-Methoxyphenylselanyl)-7-methyl-3-nitro-imidazo[1,2-a]pyridine (**5h**):* Yield: 78%, yellow solid, m.p.: 184$^0$C, $^1$H NMR (400 MHz, $CDCl_3$) δ (ppm): 9.27 (d, *J* = 7.0 Hz, 1H), 7.66 (d, *J* = 8.8 Hz, 2H), 7.38 (s, 1H), 7.08 – 6.78 (m, 3H), 3.86 (s, 3H), 2.47 (s, 3H); $^{13}$C NMR (100MHz, $CDCl_3$) δ(ppm): 160.6, 152.8, 147.8, 143.5, 137.9, 126.8, 117.7, 116.1, 115.1, 55.3,

21.6; IR(neat, ν $cm^{-1}$) 3042, 1636, 1448, 1374, 1323, 1202, 842, 520, 439 ES-MS: m/z 364.0 $[M+H]^+$

*4.1.10 2-(Mesitylselanyl)-7-methyl-3-nitro-imidazo[1,2-a]pyridine (**5i**):*Yield: 83%, yellow solid, m.p.: 177$^0$C, $^1$H NMR (400 MHz, $CDCl_3$/DMSO-$d_6$) δ (ppm): 9.17 (d, *J* = 7.0 Hz, 1H), 7.42 (s, 1H), 7.10 (dd, *J* = 7.0 Hz, 1.4 Hz, 1H), 6.94 (s, 2H), 2.38 (s, 3H), 2.33 (s, 6H), 2.24 (s, 3H); $^{13}$C NMR(100MHz, $CDCl_3$/DMSO-$d_6$) δ (ppm): 150.7, 147.2, 143.9, 143.0, 139.0, 128.4, 126.8, 124.3, 117.8, 115.3, 23.6, 21.0, 20.6; IR(neat, ν $cm^{-1}$) 2917, 1636, 1463, 1373, 1323, 1204, 1145, 840, 747, 430 ES-MS: m/z 376.2 $[M+H]^+$

*4.1.11 7-Methyl-3-nitro-2-(pyridin-2-ylselanyl)-imidazo[1,2-a]pyridine (**5j**):* Yield:76%, yellow solid, m.p.: 159$^0$C, $^1$H NMR (400 MHz, $CDCl_3$/DMSO-$d_6$) δ (ppm): 9.18 (d, *J* = 7.0 Hz, 1H), 8.48 (d, *J* = 4.1 Hz, 1H), 8.12 (d, *J* = 7.9 Hz, 1H), 7.70 (t, *J* = 7.3 Hz, 1H), 7.42 (s, 1H), 7.30–7.27 (m, 1H), 7.10 (d, *J* = 6.9 Hz, 1H), 2.43 (s, 3H); $^{13}$C NMR (100MHz, $CDCl_3$/DMSO-$d_6$) δ(ppm): 151.9, 149.5, 149.2, 147.1, 144.0, 136.7, 130.4, 126.5, 122.9, 118.1, 115.4, 21.1; IR(neat, ν $cm^{-1}$) 2951, 1640, 1466, 1443, 1325, 1142, 985, 734, 431 ES-MS: m/z 335.0 $[M+H]^+$

*4.1.12 2-(Naphthalen-1-ylselanyl)-3-nitro-imidazo[1,2-a]pyridine (**5k**):* Yield 78%, light yellow solid, m.p.: 246$^0$C, $^1$H NMR (400 MHz, $CDCl_3$/DMSO-$d_6$) δ (ppm): 9.40 (d, *J* = 6.9 Hz, 1H), 8.24 (d, *J* = 8.3 Hz, 1H), 8.08 (t, *J* = 8.3 Hz, 2H), 7.98 (d, *J* = 7.5 Hz, 1H), 7.67–7.63 (m, 1H), 7.59–7.57 (m, 2H), 7.55 – 7.54 (m, 1H), 7.51 (ddd, *J* = 8.2, 6.9, 1.4 Hz, 1H), 7.34 (td, *J* = 7.0, 1.2 Hz, 1H); $^{13}$C NMR(100MHz, $CDCl_3$/DMSO-$d_6$) δ (ppm): 150.2, 146.8, 136.6, 134.8, 133.7, 132.0, 130.7, 128.3, 127.8, 127.6, 126.2, 125.8, 124.8, 116.5, 116.0; IR (neat, ν $cm^{-1}$) 1628, 1448, 1329, 1118, 922, 742, 577 ES-MS: m/z 370.0 $[M+H]^+$

*4.1.13 4-(3-Nitro-imidazo[1,2-a]pyridin-2-ylselanyl)-N,N-dimethylbenzenamine (**5l**)*: Yield 74%, red solid, m.p.: 230$^0$C, $^1$H NMR (400 MHz, DMSO) δ 9.35 (d, *J* = 6.9 Hz, 1H), 7.77 – 7.75 (m, 2H), 7.50–7.48 (m, 2H), 7.39 (td, *J* = 6.7, 1.9 Hz, 1H), 6.80– 6.76 (m, 2H), 2.98 (s, 6H)); $^{13}$C NMR (75MHz, $CDCl_3$/$CCl_4$) δ (ppm):181.0, 137.9, 128.4, 117.2, 114.9, 113.2, 40.4; IR (neat, ν $cm^{-1}$) 3092, 2876, 1624, 1438, 1319, 1188, 1060, 916, 742, 576 ES-MS: m/z 363.1 $[M+H]^+$

*4.2 X-ray crystallographic studies*

The X-ray single crystal data of **5a**, **5d** and **5e** were collected with monochromated Mo-Kα radiation (λ = 0.71073 Å) on a Bruker SMART Apex II diffractometer equipped with a CCD area detector at 180(2) K. The crystals were positioned at 40 mm from the CCD and the spots were measured using a counting time of 5s for **5a** and **5e**, and 10 s for **5d**. Data reduction of each

compound was carried out using the SAINT-NT software package. Multi-scan absorption correction was applied to all intensity data using the SADABS programme. The structures were solved by a combination of direct methods and subsequent difference Fourier syntheses followed by successive refinements by full matrix least squares on F2 using the SHELX-2013 suite. The hydrogen atoms were inserted at ideal geometric positions and refined with $U_{iso}$ =1.2$U_{eq}$ of the parent carbon atom. Molecular and the crystal packing diagrams were drawn with the Mercury software package. The crystal data together with pertinent refinement details are summarized in Supporting Information, Table S1. The crystal structures were deposited with the Cambridge Crystallographic Database Centre (CCDC) and given the numbers CCDC 1447675-1447677.

*4.3 Computational studies*

The ground state geometries of all the synthesized compounds were optimized at the [B3LYP/6-31G(d)] level of theory without any symmetry restriction. All calculations were performed with Gaussian 03 software package [28].

*4.4 Antimicrobial studies*

The bacterial strains were grown overnight and were diluted in Mueller–Hinton broth to a cell density of $10^5$ CFU (colony forming unit)/ml. 100µl of this culture and compounds **5a-l** (80 µg/ml to 0.035µg/ml) were added into the 96-well flat bottomed microtiter plate (HiMedia, India). The plate was incubated at 37ºC without shaking for 25h. The visual and optical density at 600nm was measured using microplate reader (BioRed, Model 680). The antifungal activities against fungal species were performed according to the Clinical and Laboratory Standards Institute (CLSI, formerly NCCL) M-27-A3 and M-38-A2 in RPMI-1640 medium by broth microdilution methods. The concentrations of compounds **5a-l** ranged between 0.035µg/ml and 80µg/ml. The 96 well flat bottom microtiter plates were incubated without shaking at 30°C for 48 h. The visual and optical density was determination at 492 nm using a microplate reader (BioRed, Model 680) were used for growth inhibition.

*4.4.1 Time Kill assay analysis*

*E. coli* cells (~1 x $10^5$ CFU/ml) were inoculated in MHB medium containing **5a** (2.48 µg/ml). The tube were incubated (37°C; 200rpm) and 100 µl aliquots were removed at pre-determined time points (0, 4, 8, 12, 16, 20 and 24 h). The aliquots were serially diluted (10 fold) in saline and plated on the MHA agar plates. The numbers of colonies were counted after incubating the plates at 30°C for 25h. Similarly *C. krusei* cells (~1 x $10^4$ CFU/ml) were

inoculated in RPMI-1640 medium containing **5e**. The tubes were incubated (30°C; 200 rpm), and 100 µl aliquots were removed at pre-determined time points (4, 8, 12, 16, and 24 h).

*4.4.2 Synergy studies*

The interaction of compound **5a** with well-known antibacterial drugs Kanamycin and Rifampicin; compound **5e** with antifungal drugs Amphotericin B and Fluconazole (at sub MIC) were evaluated by the checkerboard method and expressed as the fractional inhibitory concentration index (FICI). The FICI was interpreted as synergistic when it was ≤ 0.5, as antagonistic when > 4.0, and any value in between as indifferent.

*4.4.3 FE-SEM analysis*

*E. coli* and *C. krusei* cell suspensions from overnight grown cultures were prepared in MHB and RPMI-1640 medium (pH 7) respectively. Compound **5a** (at 2.48µg/ml) was added to the *E. coli* cells (~1 x $10^5$ CFU/ml), whereas **5e** (at 9.96 µg/ml) was added to the *C. krusei* (~1 x $10^4$ CFU/ml) and incubated at 30°C for 2h.

*4.4.5 Cytotoxicity analysis*

Cytotoxicity analysis of compounds **5a**, **5e** and **5j** against HEK-293 (normal human embryonic kidney cells) and HeLa (cervical cancer cells) by done using MTT (3-(4,5)-dimethylthiazol-2-yl)-2,5-diphenyl tetrazolium bromide) protocol. Briefly, the cells ($5x10^4$ /well) were cultured in RPMI-1640 medium supplemented with 10% fetal bovine serum in 96-well microtiter plate at 37ºC for overnight. The next day, compounds **5a**, **5e** and **5j** at MIC were added to the cells in separate wells and incubated at 37ºC for 18 hours. The cells were further incubated at 37ºC for 3 to 5h in 20µl of MTT solution (5 mg/ml) in PBS. The supernatant (120µl) was removed, 100µl DMSO was added, and the resulting suspension was mixed to dissolve the formazan crystals. The percent viability of cells was calculated by the ratio of $O.D_{570}$ of treated cells to the $O.D_{570}$ of untreated cells. Untreated cells and 10% dimethyl sulfoxide (DMSO) were taken as negative and positive control respectively.

**Acknowledgements**

This work is supported by Science and Engineering Research Board (SERB), India (grant no. SB/SO/BB/0040/2013), Department of Science and Technology (DST-PURSE), India, BiMED-Institute of Biomedicine (FCT Ref. UID/BIM/04501/2013) and CICECO-Aveiro Institute of Materials (FCT Ref. UID/CTM/50011/2013). SK and NS thank CSIR, New Delhi, India for their

research fellowships (grant no. 09/135/(0674)/2012/EMR-I and 09/135(0675)/2012-EMR-I). KKB is grateful to CSIR, India for Emeritus Scientist Scheme India 21(0967)/13/EMR-II.

**References**

[1]. G. Mugesh, W. W. D. Mont, H. Sies, Chem. Rev. 101 (2001) 2125–2179

[2]. L. Orian, S. Toppo, Free Radical Biology and Medicine 66 (2014) 65–74

[3]. a) T. Nishiyama, K. Tokunga, Org. Lett. 1 (1999) 1725–1727; b) T. Nishino, M. Okada, T. Kuroki, J. Org. Chem. 67 (2002) 8696–8698; c) B. C. Ranu, T. Mandal, J. Org. Chem. 69 (2004) 5793–5795; d) O. E. D. Rodrigues, K. Gul, A. L. Braga, J. Org. Chem. 75 (2010) 3886–3889; e) V. P. Reddy, A. V. Kumar, K. R. Rao, Org. Lett. 11 (2009) 951-953; f) N. Taniguchi, J. Org. Chem. 72 (2007) 1241–1245; g) X. Zhao, Z. Yu, S. Nu, R. Lu, W. J. He, Org. Chem. 70 (2005) 7338–7341; h) K. Ajiki, M. Hirano, K. Tanaka, Org. Lett. 7 (2005) 4193–4195.

[4]. M. Godoi, E. W. Ricardo, G. V. Botteselle, F. Z. Galetto, J. B. Azeredo, A. L. Braga, Green Chem. 14 (2012) 456–460.

[5]. D. Alves, S. Thurow, R. Webber, G. Perin, E. J. Lenardão, Tet. Lett. 54 (2013) 3215–3218.

[6]. S. Banerjee, L. Adak, B. C. Ranu, Tet. Lett. 53 (2012) 2149–2152.

[7]. S. Thurow, F. Penteado, G. Perin, R. G. Jacob, D. Alves E. J. Lenardão, Green Chem. 16 (2014) 3854–3859.

[8]. C. W. Nogueira, G. Zeni, J. B. T. Rocha, Chem. Rev. 104 (2004) 6255–6285

[9]. S. Kumar, J. Yan, J. Poon, V. P. Singh, X. Lu, M. K. Ott, L. Engman, S. Kumar, Angew. Chem. Int. Ed. 55 (2016) 3729 –3733

[10]. J. E. Cone, R. M. D. Rio, J. N. Davis, T. C. Stadtman, Proc. Natl. Acad. Sci. USA 73 (1976) 2659–2663.

[11]. A. Bock, K. Forchhammer, J. Heider, W. Leinfelder, G. Sawers, B. Veprek, F.Zinoni, Molecular Microbiology 5 (1991) 515–520.

[12]. M. Ninomiya, D. R. Garud, M. Koketsu, Coord. Chem. Rev.255 (2011) 2968–2990.

[13]. F. M. Libero, M. C. D. Xavier, F. N. Victoria, P. S. Nascente, L. Savegnago, G. Perin, D. Alves, Tet. Lett. 53 (2012) 3091–3094

[14]. Victoria, C. S. Radatz, M. Sachini, R. G. Jacob, D. Alves, L. Savegnago, G. Perin, A. S. Motta, W. P. Silva, E. J. Lenardão, Food Control 23 (2012) 95–99.

[15]. D. Plano, D. N. Karelia, M. K. Pandey, J. E. Spallholz, S. Amin, A. K. Sharma, J. Med. Chem. 59 (2016) 1946–1959

[16]. F. M. Ramos, H. S. Zamora, M. E. C. Aldrete, E. M. Camargo, Y. M. Flores, M. S. García, Eur. J. Med. Chem. 43 (2008) 1432–1437.

[17]. M. A. F. Herrera, J. S. Ramírez, L. S. Sánchez, H. L. Muñoz, M. L. E. Sánchez, Eur. J. Med. Chem. 74 (2014) 451–460.

[18]. Z. Al-Eisawi, C. Stefani, P. J. Jansson, A. Arvind, P. C. Sharpe, M. T. Basha, G. M. Iskander, N. Kumar, Z. Kovacevic, D. J. R. Lane, S. Sahni, P. V. Bernhardt, D. R. Richardson, D. S. Kalinowski, J. Med. Chem. 59 (2016) 294–312

[19]. H. Zeng, J. He, D. Li, K. Xiong, G. Zhang, Bioorg. Med. Chem. 20 (2012) 3816–3827.

[20]. a) G. Kedarnath, V. K. Jain, Coord. Chem. Rev. 257 (2013) 1409–1435; b) A. K. K. Bhasin, C. Jacob, F. Sasse, K. Karaghiosoff, K. K. Bhasin, S. K. Mehta, A. Sharma, Rishu Design, J. Organomet. Chem, 785 (2015) 19–25; c) L. Savegnago, A. I. Vieira, N. Seus, B. S. Goldani, M. R. Castro, E. J. Lenardão, D. Alves, Tet. Lett. 54 (2013) 40–44; d) B. Wang, P. Li, F. Yu, P. Song, X. Sun, S. Yang, Z. Lou, Han, K. Chem. Commun. 49 (2013)1014–1016 e) R. A. Hussain, A. Badshah, J. M. Pezzuto, N. Ahmed, T. P. Kondratyuk, E. Park, Journal of Photochemistry and Photobiology B: Biology 148 (2015) 197–208; f) Z. Wen, J. Xu, Z. Wang, H. Qi, Q. Xu, Z. Bai, Q. Zhang, K. Bao, Y. Wu, W. Zhang, Eur. J. Med. Chem. 90 (2015) 184–194; g) A. S. Hodage, P. P. Phadnis, A. Wadawale, K. I. Priyadarsini, V. K. Jain, Org. Biomol. Chem. 9 (2011) 2992–2998.

[21]. J. P. Paolini, R. K. Robins, J. Org. Chem. 30 (1965) 4085-4090.

[22]. A. K. Bagdi, S. Santra, K. Monir, A. Hajra, Chem. Commun. 51 (2015) 1555–1575.

[23]. J. Rafique, S. Saba, A. R. Rosario, A. L. Braga, Chem. Eur. J. 22 (2016) 1–10

[24]. a) K. S. Gudmundsson, J. D. Williams, J. C. Drach, J. Med. Chem. 46 (2003)1449–1455; b) M. Lhassani, O. Chavignon, A. Gueiffier, Eur. J. Med. Chem. 34 (1999) 271–274; c) Y. Rival, G. Grassy, A. Taudou, R. Ecalle, Eur. J. Med. Chem. 26 (1991) 13–18; d) P. C. Lima, M. A. Avery, B. L. Tekwani, C. A. M. Fraga, IL Farmaco57 (2002) 825–832; e) L. Paloque, M. Laget, A. Cohen, N. Azas, P. Vanelle, Bioorg. Med. Chem. 21 (2013) 7155–7164; f) B. D. Maxwell, O. G. Boye, K. Ohta, J. Label. Compd. Radiopharm. 48 (2005) 397–406; g) A. Kamal, J. S. Reddy, M. J. Ramaiah, Med. Chem. Commun. 1 (2010) 355–360; h) A. T. Baviskar, C. Madaan, R. Preet, P. Mohapatra, V. Jain, A.

Agarwal, S. K. Guchhait, J. Med. Chem. 54 (2011) 5013–5030; i) R. B. Lacerda, D. Lima, D. Silva, Bioorg. Med. Chem. 17 (2009) 74–84.

[25]. Tisler, M. Pure & Appl. Chem. 52 (1980) 1611–1621.

[26]. M. A. Bazin, S. Marhadour, A. Tonnerre, P. Marchand, Tet. Lett. 54 (2013) 5378-5382.

[27]. H. J. Reich, M. L. Cohen, P. S. Clark, Org. Synth. 6 (1988) 533-535.

[28]. P. J. Stephens, F. J. Devlin, C. F. Chabalowski, M. J. Frisch, J. Phys. Chem., 98 (1994) 11623–11627.

[29]. J. S. Dhau, A. Singh, A. Singh, B. S. Sooch, P. Brandão, V. Félix, J. Organomet. Chem. 766 (2014) 57-66.

## Highlights

- Synthesis of novel imidazo[1,2-*a*]pyridine based organoselenium compounds is achieved.
- Structural characterization is performed using X-ray and computational analysis.
- The antimicrobial evaluation using time kill assay and FE-SEM analysis gave good results.
- The synergistic studies with antibiotics exhibit enhanced antimicrobial activity.